



The Path to Flight: Integration & Testing Updates from the Alpha CubeSat Mission

Apurva Hanwadikar^{a,*}, Italivi Diaz^a, Adiba Sajed^a, Cion Kim^a, Langston Johnson^a, Verena Padres^a, Damian Hackett^a, Joshua Umansky-Castro^a, Andrew Filo^b, Alex Burke^c

^aSibley School of Mechanical and Aerospace Engineering, Cornell University, Ithaca NY, United States

^b4Special Projects, Cupertino CA, United States

^cIndependent Researcher, Pacifica CA, United States

Abstract

Alpha is a 1U CubeSat developed at Cornell University to demonstrate the deployment of a retroreflective light sail in low Earth orbit. The mission utilizes lightweight ChipSats for sensing and communication, which are mounted directly on the sail. While earlier prototypes confirmed basic functionality, this paper focuses on the final integration, testing, and validation needed to prepare the spacecraft for launch. We present key design efforts across mechanical, electrical, and software subsystems, including tolerancing of mechanical components, iterative development of sail-mounted antennas, and updates to the CAD and Bill of Materials (BOM) for mass property verification. Environmental tests, including thermal vacuum and vibration tests, were conducted to verify physical performance under flight conditions. A high-altitude balloon mission was also used to validate antenna performance at a near-orbital distances. Procedures for permanent flight assembly were developed to ensure repeatability and consistency. The results demonstrate that subsystem-level functionality does not guarantee system-level readiness and that achieving launch qualification requires comprehensive and integrated testing. This work outlines the process of refining research hardware into flight-ready systems, contributing to broader efforts in low-cost spacecraft development.

Keywords: CubeSat, ChipSat, light sail, solar sail, High Altitude Balloon

1. Introduction

Cornell University is now launch-ready for Alpha, a 1U CubeSat that will deploy a retroreflective light sail in low Earth orbit. Unlike other solar sail missions, Alpha's sail is both free-flying and miniaturized[1]. The payload consists of ChipSats, chip-scale spacecraft mounted directly to the sail, that will deploy with it and handle sensing, processing, and communication. Their small size and mass make them well-suited for propulsion by a compact sail.

While earlier work focused on developing Alpha into a functional prototype, achieving launch readiness required a more thorough process: testing under realistic conditions, refining hardware for integration, and verifying that everything would withstand the space environment. Many components worked fine individually, but introducing full-system interactions often revealed

new problems, including interference, thermal shifts, and mechanical tolerance issues, that only became apparent during integrated testing.

This paper describes the work done to close that final gap between a working prototype and a launch-approved satellite. In addition to the behavior and performance of individual components, such as sail-mounted antennas, we detail the full spacecraft qualification process, which includes thermal vacuum and vibration testing, iteration of mechanical components like deployment switches, finalization of CAD and the bill of materials, and development of flight assembly procedures. We also include the integration and validation of mission software across the CubeSat's electrical systems. Each section focuses on a different part of what it took to get Alpha flight-ready, both technically and procedurally. The goal is to demonstrate how small, easily overlooked details, such as mechanical clearances, component integration, RF interference, or screw length, can make or break a mission, and how the team worked

*Apurva Hanwadikar, aah246@cornell.edu

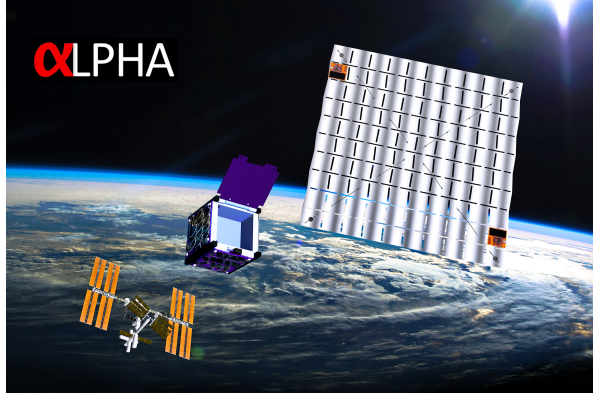


Figure 1: Alpha Mission Launch poster with the CubeSat deploying a light sail with ChipSats attached at each corner.

through these challenges to build a fully functioning spacecraft.

2. Mechanical Design

2.1. Design and Manufacturing

Before Alpha could be cleared for flight, every mechanical subsystem needed to meet strict tolerances, especially those interfacing with the deployer. One of the most critical components among these was the deployment switch plunger system (Figure 2), which ensures the CubeSat remains powered off until it is safely ejected into orbit.

A common requirement for CubeSats being transported within a CubeSat Deployer, such as Alpha with the NanoRacks CubeSat Deployer (NRCSD), is that they remain completely powered off during the transport and launch of the deployer. To ensure that this requirement is met with some fault tolerance, three limit switches are present within the CubeSat that directly cut power to the satellite when pressed. For Alpha, the interface between each limit switch and the surrounding NRCSD is a custom-designed plunger, which nominally protrudes beyond the standard 1U dimensions of the CubeSat. When Alpha is installed into the NRCSD among the other CubeSats, the plungers are forced into the body of the CubeSat, each pressing its respective limit switch to ensure the CubeSat remains in a powered-off state. Figure 3 displays the CubeSat in its stowed state within the NRCSD during a fit check.

Even though most of our mechanical components were technically “functional” in earlier builds, getting them to a point where we could trust them in space

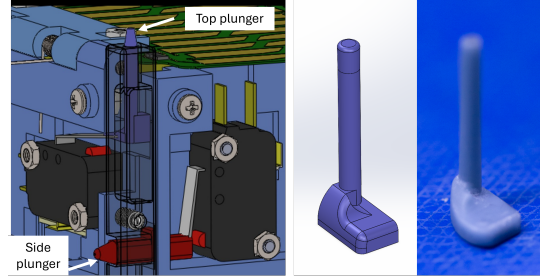


Figure 2: Cutaway view of deployment switch plungers embedded within CubeSat rails (left) and close-up view of finalized top plunger Flight Unit (right)

required far more work than expected. The custom-designed deployment switch plungers, like many moving parts on the spacecraft, had to meet tight tolerances to be both reliable and fault-tolerant under launch loads. A mishap with any one of the plungers — getting stuck, missing the switch, or failing to depress completely — could lead to a power failure on orbit, creating a single point of failure for the mission. The 3D-printed plungers are a good example of the mechanical iteration and attention to detail that were needed across many parts of the spacecraft.

To validate the custom plunger designs, the team performed extensive testing using prototype plungers 3D-printed on an in-house resin printer. The resin printer was important for enabling rapid iteration and small design modifications, while maintaining the prototypes’ close resemblance to the flight hardware. Standard 3D-printers using fused deposition modeling (FDM) typically have looser tolerances when evaluated against the source model dimensions compared to similarly priced resin printers. That difference was one of the reasons we selected resin printing. Additionally, the smooth surface finish of the resin prints was more representative of the expected finish of the final Accura® Bluestone™ flight units.

Each prototype plunger was installed in the flight unit for testing. Originally, the EDU was used for this purpose, but we found that the EDU chassis had less precisely manufactured hardware compared to the flight unit. Testing on the actual flight hardware proved essential to determine the correct final dimensions for each plunger.

Once installed, we checked four things: whether the plunger fully depressed the limit switch, whether there was a risk of slipping off the switch lever, whether the plunger was flush with the chassis when fully depressed, and whether it could get stuck if pushed at an off an-

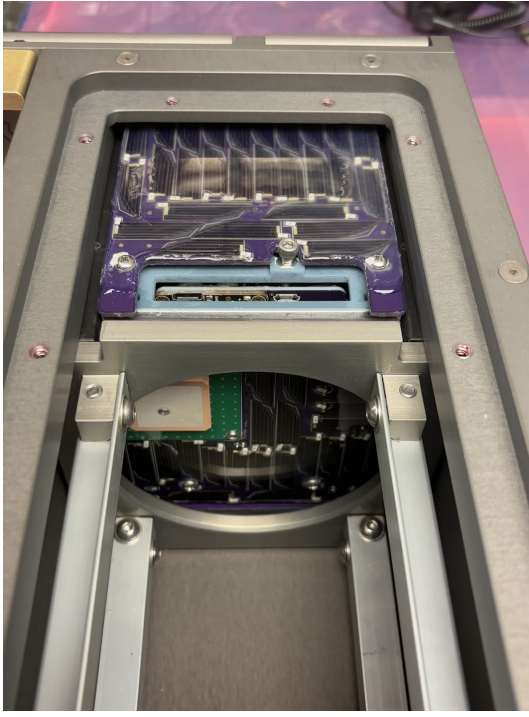


Figure 3: The CubeSat in the NanoRacks deployer.

gle. These checks helped catch flaws in each iteration, and we repeated them in every version. Once the ideal dimensions were confirmed using the resin prototypes, we ordered slightly oversized Bluestone™ versions and carefully sanded each one down to the correct dimensions. Several iterations of the SLA prints were still required due to tolerancing discrepancies compared to both the resin prints and the original CAD model.

With these final adjustments, we were confident the plungers would perform reliably under both vibrational stress and the tight mechanical constraints imposed by the NRCSD. Ultimately, designing the plungers was about layers of iteration and prototyping. We spent weeks refining prints, adjusting lever interfaces, and inspecting angles under magnification. That same process of taking parts that seemed “fine” and making them actually flight-ready was repeated for doors, hinges, latches, antennas, and more. In the case of small spacecraft, such as CubeSats, tolerance stackups can easily lead to larger fit issues. Working at this level of detail on individual components is essential to ensure that the entire system fits and functions correctly.

Part number	Part Name	Use	Group	Qty	Unit Mass (g)	Geom (l x w x h) (mm)	CAD Measured Volume (mm ³)	Density (kg/m ³)	Material(s)
CubeSat Body									
1	Total Mass			1171.02	g				
31	Main Chassis	Primary Str 1		253.93	73x75x2	150x48	1.688669	Accur® Bluestone™	
32	Sail Compartment Plate	Primary Str 1		17.66	73x75x2	30x42	1.683221	Accur® Bluestone™	
33	M3 31mm Hex Standoff	Primary Str 4		6.15	6x6x31	0.89	6.910112	18-8 Stainless Steel	
34	M3 31mm Hex Standoff	Primary Str 4		1.78	6x6x31	0.24	7.248124	18-8 Stainless Steel	
35	Bottom Plate	Primary Str 1		16.25	100x100x0.762	4.9	3.316327	Al 6061 T6 Hard Anod	
36	Rail (SW, NE)	Rail with no deployment sw Primary Str 2		21.95	8.54x5x113.5	7.97	2.754078	Al 6061 T6 Hard Anod	
37	Rail (SW)	Rail with 2 deployment sw Primary Str 2		19.97	8.54x5x113.5	6.59	2.759328	Al 6061 T6 Hard Anod	
38	Rail (NW)	Rail with 2 deployment sw Primary Str 1		18.22	8.54x5x113.5	6.68	2.773745	Al 6061 T6 Hard Anod	
Door Assembly									
39	Torsion Spring (Left Wound)	Door Assen 1		0.32	0.58x112.5x38	0.04	8	Music-Wire Steel	
40	Torsion Spring (Right Wound)	Door Assen 1		0.32	0.58x112.5x38	0.04	8	Music-Wire Steel	
41	Door Latch	Door Assen 1		0.29	2x6x1	0.2	3.1	Ceramic	
42	Rod for Door Latch	Door Assen 1		0.29	2x6x1	0.2	1.45	Carbon Fiber	
43	Lateral Compression Spring	Door Assen 1		1.46	0.6x0.6x29	0.05	29	Stainless Steel	
44	Door Push Pins	Door Assen 1		0.01	2.5x2x0.5	0.16	1.783714	Brass/Steel/Copper	
45	Door Latch	Door Assen 1		4.93	17.6x5.5x16.5	3.32	1.684644	Accur® Bluestone™	
47	Door Latch	Door Assen 1		6.64	16.8x20x18.5	4.94	3.054444	Al 6061 T6 Hard Anod	
48	Burn Wire	Door Assen 1		0.12	0.7x0.5x0.5	N/A	3.32	Carbon Fiber	
49	2.54mm Male Header Pins	Cuts fishing line to open dos Door Assen 4		0.05846	0.26x1x0.40	N/A	7.866	Nichrome	
		Nichrome wire wrapped to 1 door Assen 4		0.055598	2.5x3x1.15	0.0597	2.830079	Polybutene Thermofix	
Payload Sub-Components									
50	TMP38 Temperature Sensor	Monitors battery temperature Payload Sub 1		0.21	4.5x4x0.5	0.11	1.909091	Plastic, Copper, Silicon	
51	Photodiode	Verifies sail extended compact Payload Sub 1		0.24	5x4x1x1.8	0.06	4	Ceramic, CdS, Copper	
52	Optical Deployment Sensor (PTCD)	Verifies sail unfolding Payload Sub 1		2.27	28x19.8x5.78	1.45	1.565117	PCB, FR4, Copper, Plat	
53	IE Rail Top Plunger	Verifies rail top height Payload Sub 1		0.12	4.5x4x0.5	0.06	1.565117	PCB, FR4, Copper, Plat	
54	Short Lead Weight	For use on a face, under des Payload Sub 1		2.337268	6.5x14.7x2.15	0.20613125	11.34	Lead	
Chassis-Mounted Peripherals									
55	Short-Arm Deployment Switch	Cuts off battery power when Chassis-Mo 1		7.9	59.8x15.7x9.58	4.45	1.783296	PCT/Polyester/Aluminum	
56	Long-Arm Deployment Switch	Cuts off battery power when Chassis-Mo 2		8.08	59.8x15.7x9.58	4.45	1.870523	PCT/Polyester/Aluminum	
57	IE Rail Side Plunger	Verifies rail side height Chassis-Mo 1		0.12	24.0x4x1.5	0.08	0.31851	1.788043	Accur® Bluestone™
58	NW Rail Side Plunger	Chassis-Mo 1		0.96	21.0x6.5x49.4x94	0.37562	1.667767	Accur® Bluestone™	
59	IE Rail Top Plunger	Chassis-Mo 1		0.96	24.0x5x4.5x14	0.17	1.637228	Accur® Bluestone™	
60	MonelMetal Rod	Magnetoperquer copper coil Chassis-Mo 3		6.93023	10.5x1.5x10.5x9.9	0.532457981	8.950029	MonelMetal (nickel-chromium-iron)	
61	Magnetoperquer Mounts	Chassis-Mo 3		6.086619	5.5x15x18.8	0.48	8.759983	MonelMetal (nickel-chromium-iron)	
62	Steel Strength	Chassis-Mo 3		12.47	15x15x8	1.72	1.686649	Accur® Bluestone™	
		Small RFB Switch		1.12	2.4x2.4x1	0.12	7.813395	313 Stainless Steel	
Battery Compartment									
64	LiPo Batteries (2000mAh 3.7V LiPoPO4) + Batteries	Battery Cor 2		40.74	61.0x49.7x6.07	20.18	2.018831	LiPoPO4; Aluminum f	
Avionics Stack									
65	Top Antenna Adapter	Top Anten 1		25.85	40x14x45x1.55mm	8.73	2.945054	PCT/Polyester/Aluminum	
66	RockBLOCK 4000 (M2U) Radio	Radio Transceiv 1		60.00	100x100x10	33.58	1.886957	PCT/Poly, Copper, PCB	
67	RockBLOCK spacer	Support between RockBLOCK Top Anten 1		1.380669	25x10x2	0.7	1.683669	Accur® Bluestone™	
68	SMA to 1.7L Adapter	Top Anten 1		2.13	8.4x8.0x8.0	0.423597	5.027713	Brass/Stainless Steel/G	
69	1.7L to SMA Adapter	Top Anten 1		2.13	8.4x8.0x8.0	0.54	5.285714	Brass/Stainless Steel/G	
70	2-pin JST Pin Connector (M, Right-angle)	Battery Connecto 1		0.13	2.0x4.5x8.0	0.09	1.644464	Polyamide (Nylon)	
71	Small RFB Switch	Disconnects batteries during Top Anten 1		1.86	19.8x10.3x8	1.19	1.563052	PCT Polyester/Aluminum	
		Small RFB Switch		1.12	2.4x2.4x1	0.12	1.654542	Brass/Stainless Steel	

Figure 4: Sample of full CubeSat Bill of Materials.

2.2. CAD and BOM Work

Updating the CAD and matching it to the finalized Bill of Materials (BOM) was one of the more time-consuming but important steps in preparing for flight. The goal was to ensure the model accurately represented every detail, including fasteners, coatings, wire mass, and even adhesives. This level of detail was necessary for both documentation and flight analysis. A complete and accurate BOM gave us a precise inventory of every component used in the flight unit, while the CAD model allowed us to extract the total mass, center of gravity, and moments of inertia needed for attitude control simulations. To update the BOM, each component of the spacecraft was measured and weighed individually. The dimensions were then used to estimate component surface area for verification of NanoRacks outgassing requirements and volume in simulations for NASA-KSC’s orbital debris assessment report ODAR). For more intricate shapes with downloadable CAD models (e.g. screws from McMaster-Carr), software-calculated volumes and surface areas were used instead. The BOM was reorganized to logically reflect the physical layout of the spacecraft, divided into functional categories: ChipSat-Sail Payload, CubeSat Body, which was further subdivided into Primary Structural Components, Door Assembly, Payload Sub-Compartments, Chassis-Mounted Peripherals, and Battery Compartment. It also included the Avionics Stack, Solar Panel Assembly, fasteners and wiring, as well as miscellaneous items such as epoxy, Loctite®, and wires. Figure 4 displays a sample of the final-

ized BOM. The full set of data points includes: Part number, Part name, CubeSat Part Code, Subsystem Code, Part Use/Function, Group/Category Name, Quantity, Unit Mass, Unit Volume, Density, Component Materials, Manufacturer, Manufacturer Product Number, Supplier, Supplier Product Code, Purchasing Link, Datasheet Link, Online Tutorial Link (if available), and Additional notes.

The CAD modeling process for the Alpha CubeSat began with a comprehensive review of the existing assembly to identify inconsistencies, missing components, and areas requiring design updates. An exploded view of the complete assembly was used to visualize the relationships between parts and evaluate component integration. The components and subassemblies of the model were reorganized to match the categories set in the BOM. This reorganization enabled more efficient navigation of the digital model, streamlined subassembly updates, and improved traceability between CAD and hardware components. A critical outcome of this rework was the synchronization of the CAD model with the finalized Bill of Materials (BOM), ensuring that all mechanical and electrical design revisions were accurately reflected in both documentation and the 3D model.

CAD updates also included the integration of smaller components that were previously missing, such as copper magnet wire, electrical connectors (e.g., JST headers, 20-pin crimp housings), solar panel stringers, and additional hardware, including spacers, washers, and O-rings. Numerous part dimensions were revised, including hole placements, fastener lengths, and latch geometry. Mass values were added or corrected for all components, including minor elements such as diodes and resistors, based on the finalized BOM spreadsheet. Special attention was paid to electrical subsystem additions such as the solar panels and avionics stack, which were updated with precise weightings for conformal coating and wire mass distribution. Mass properties were validated at both the subassembly and full assembly levels, with the goal of ensuring the CAD model accurately represented the CubeSat's actual mass. The final CAD mass matched the BOM-derived mass within 1 gram of tolerance, allowing for accurate extraction of mass properties and moments of inertia.

Matching the CAD model to the flight configuration enabled high-fidelity calculations of the spacecraft's inertia tensor, used for dynamic simulations and planning of attitude control. Mass distribution refinements, including ballast placement and wire routing, were made in accordance with the major-axis rule to align the CubeSat's maximum principal axis of inertia with the

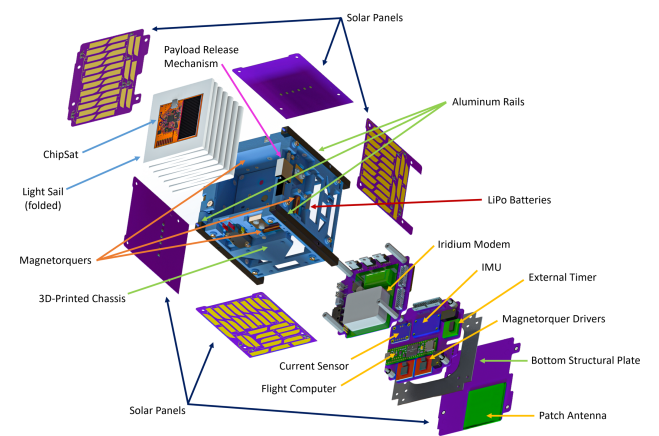


Figure 5: Annotated exploded view of CubeSat CAD model [Courtesy of Richard Zheng '25].

geometrical z-axis, along which the solar sail is deployed. These precise adjustments ensured that the mechanical design supported both the stability and performance of the spacecraft during deployment and flight operations.

Once complete, the CAD model and BOM also acted as a final cross-check before integration. Matching the measured mass gave us confidence in our inertia tensor, and the layout helped verify that all hardware fit without interference. Even minor additions, such as washers, Loctite®, or epoxy, were accounted for, avoiding last-minute surprises during flight assembly. Although incremental, these refinements were essential for ensuring that our design was fully flight-ready.

3. CubeSat Assembly

3.1. Assembly Procedure

Before we could begin assembling the flight unit, we needed a well-defined, repeatable procedure with no ambiguity about the order of operations or recommended techniques to accomplish a task. Many of the assembly steps, such as applying Loctite®, folding the sail, and staking down wires, are irreversible, so any mistake means potentially damaging flight hardware or starting over with a limited supply of spare parts. The goal of the procedure is to prevent those mistakes by documenting exactly what had to happen, when, and how it should be done (Figure 6). The availability of a clear step-by-step guide for assembly, with minimal confusion, was essential in avoiding errors.

The procedure manual included precise instructions for every stage of the assembly process, including

SSDS	OLPHA	Document description	Submission	Review	Page
		Same time triple checking that the ZIF card has been seated well			1 of 2
		Shows that the ZIF card is being checked correctly, inserted into the ZIF socket and then the ZIF card is being checked again to ensure it is seated well. This is a good step to prevent damage to the ZIF card or the ZIF socket if the ZIF card is not seated well.			2 of 2
		Note for future use, ZIF, ZIF, and ZIF for first seat reinsert ZIF and check again for fine connection			3 of 2
		Same time triple checking that the ZIF card has been seated well			4 of 2
		Note for future use, ZIF, ZIF, and ZIF for first seat reinsert ZIF and check again for fine connection			5 of 2
		Same time triple checking that the ZIF card has been seated well			6 of 2
		Note for future use, ZIF, ZIF, and ZIF for first seat reinsert ZIF and check again for fine connection			7 of 2

Figure 6: Spreadsheet highlighting iterative refinements made to the flight assembly procedure.

component alignment, torque specifications, connector orientations, and electrostatic discharge (ESD) precautions. ESD precautions were maintained by using grounding straps and conductive mats during the handling of sensitive electronics. Tests and verifications are performed after each major step to detect issues prior to further integration. Visual photos of each step, callouts, and step-by-step checklists were incorporated to assist both experienced and new team members in following the procedure correctly. Video tutorials are included for more intricate techniques. The goal was for anyone to be able to assemble the flight unit with little prior knowledge.

To validate the effectiveness of the guide and reduce the risk of errors during actual flight assembly, the team conducted multiple rehearsal builds using non-flight hardware units. These rehearsals served as both a training opportunity for the student team and a dry run to evaluate the clarity and completeness of the procedure. Throughout this process, real-time feedback was collected, and iterative revisions were made to improve the guide's usability and accuracy.

This rehearsal phase proved critical in identifying and correcting potential failure points in the workflow, including sequencing issues, missing steps, and ambiguous language. It also provided insight into the necessary tools, environmental requirements, and key considerations for the final integration. The guide was split into separate guides to sequence the process of flight assembly. There were 11 guides, including:

- Acceptance testing procedure
- Avionics stack assembly

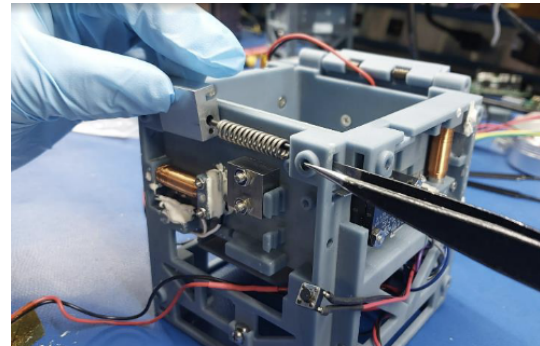


Figure 7: Documentation of assembly process for the sail compartment door latch and spring.

- Peripherals and structural assembly
- Solar panel assembly procedure
- Permanent assembly prep procedure
- Secure wiring harnesses procedure
- Top half permanent assembly procedure (Figure 7)
- Avionics stack permanent assembly procedure
- Solar panel permanent assembly procedure
- Payload integration procedure

This work was essential for ensuring the flight build could happen smoothly, without introducing risk from human error. It also provided us with a framework for tracking progress and verifying that everything was built to specification. By the time we started on the real CubeSat, we had a repeatable process in place both for Alpha's specific mechanical requirements and for future CubeSat missions requiring similar assembly techniques.

3.2. Final Assembly

Once the procedures were in place, we moved into the final integration of the actual flight unit. At this point, most of the design and subsystem-level testing had already been completed. The process was tracked through sign-off sheets and photographed step-by-step, both for traceability and so that each irreversible action could be reviewed. This phase involved the physical construction and final assembly of the flight-ready CubeSat that would be launched into orbit.

All components, ranging from structural segments and avionics boards to the light sail, were subjected

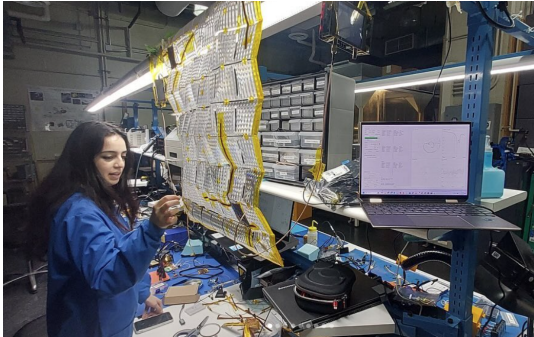


Figure 8: SSDS student Italivi Diaz tuning the ChipSat antennas while mounted to the light sail.

to thorough pre-integration inspections and functional testing prior to assembly. The assembly environment was maintained clean, and ESD control measures were implemented to protect sensitive electronics. At each critical stage of integration, specific tasks, such as connector mating, application of Loctite®, or storage of deployable elements, were verified by multiple team members and documented through photographs and sign-off logs.

Particular attention was given to mechanical fastening steps, ensuring correct torque application, and folding and storing the lightsail. Electrical subsystems were checked for continuity and signal integrity following each phase of integration. These quality measures helped ensure that no unexpected errors occurred during the build process.

Upon completion of the full-stack integration, the assembled CubeSat underwent a series of final functional and system-level tests to confirm the operability of all major subsystems. These tests were essential to validate that no faults had been introduced during the mechanical integration process and that the CubeSat was flight-ready.

By having a repeatable process for building the entire system, we had high confidence not just in the hardware but in the quality of the build process. Every step had been rehearsed, documented, and signed off which made the process reliable and comprehensive. We knew the flight unit matched our expectations because we had built it the same way multiple times before. That consistency gave us confidence that the flight unit would perform as intended once deployed.

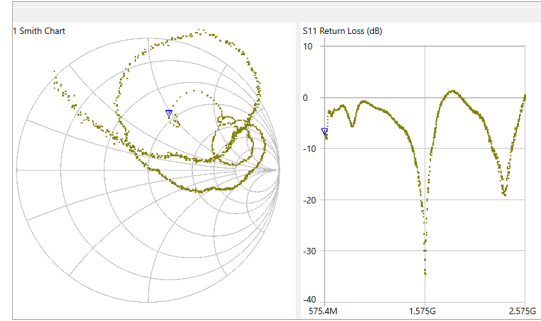


Figure 9: NanoVNA portal displaying loss as a function of frequency for a perfectly tuned GPS antenna. The graph line in the middle is the target frequency (1.575GHz for GPS). At the target frequency, the impedance should be 50 ohms, right at the center of the Smith Chart.

4. Light Sail-ChipSat Integration

With the CubeSat bus complete, it was now time to integrate the ChipSat-equipped light sail payload. In parallel to the development of the CubeSat, several years were spent designing the ChipSats that are mounted to the sail. [2]. Once the ChipSats were finalized, however, integrating the antennas onto a foldable light sail introduced new mechanical and electrical challenges. The ChipSats feature custom dipole radio antennas for downlinking data via LoRa (long-range) transceivers and a separate dipole antenna to receive GPS data for the sail. Each antenna consists of two copper dipole legs embedded within a flexible Kapton PCB substrate. The dipole legs are soldered to the main ChipSat body of the same polyimide substrate. Unlike traditional antenna deployment systems, these antennas had to be stored within the sail, survive folding and vibration, and deploy passively during sail expansion, all while meeting both RF and mechanical requirements.

We discovered that early antenna designs integrated on the light sail exhibited deployment failures and electrical inconsistencies due to origami-induced creases from the sail. These creases altered the effective electrical length of the antenna, resulting in shifted, multiple, or missing resonance peaks. These issues are often compounded as a partially unfolded antenna can shift in resonant frequency and also increase interference with an adjacent ChipSat, degrading overall performance. Mechanical failures also occurred as mechanical shearing near the pad area during folding or handling led to broken solder joints or ripped Kapton.

The key metrics, measured using a NanoVNA (Figure 9), were resonance at the target frequency and good impedance matching. For the LoRa antenna, ideal res-

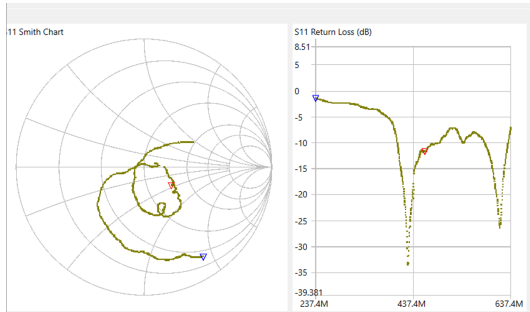


Figure 10: NanoVNA graph for a slightly shifted LoRa antenna after sail folding.

onance occurs at 437.4 MHz, with acceptable performance indicated by a return loss of -15 dB to -20 dB (corresponding to a signal power transmission of 96.8 to 99.0 percent) (Figure 10). For GPS antennas (1575.42 MHz), which operate at higher frequencies, the requirements are stricter, typically set at a level below -20 dB, to account for GPS signals being inherently weaker and the antennas having narrow bandwidths (Figure 9).

Tuning was performed by incrementally trimming the antenna elements and monitoring shifts in the resonant peak. Following the inverse relationship $f = c/\lambda$, a shorter dipole corresponds to a higher resonant frequency. For increased accuracy, the sail (and antenna legs) we pre-folded and stowed in the CubeSat prior to trimming. During tuning, the ChipSats were also mounted to the sail, which in turn was suspended in the air as shown in Figure 8.

After iterating on various design options with different geometries, angles, copper thickness, substrate materials, and stiffening mechanisms, we settled on a hybrid solution that combined two flexible laminated antennas with mechanically reinforced antennas utilizing nitinol hinges (Figure 14).

The flexible antennas were made from Kapton-based PCB material that conforms to the shape of the sail. We laminated the antennas onto the sail folds, and they naturally expanded outward when the sail deployed (Figure 11). However, for them to work, the dipoles had to lie flat along the plane of the sail, pointing inward toward the center, which only worked with two ChipSats placed diagonally from each other.

The hinged antennae were constructed using rigid PCB sections joined by flexible nitinol hinges, allowing for folding (Figures 12 and 13). Nitinol's shape-memory properties provided a passive deployment mechanism, allowing the antenna to unfold.



Figure 11: Flexible antenna laminated onto the sail in the flight configuration.

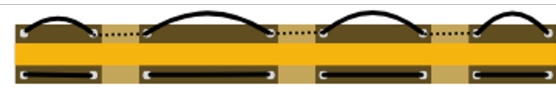


Figure 12: Concept for nitinol-straightened hinges.

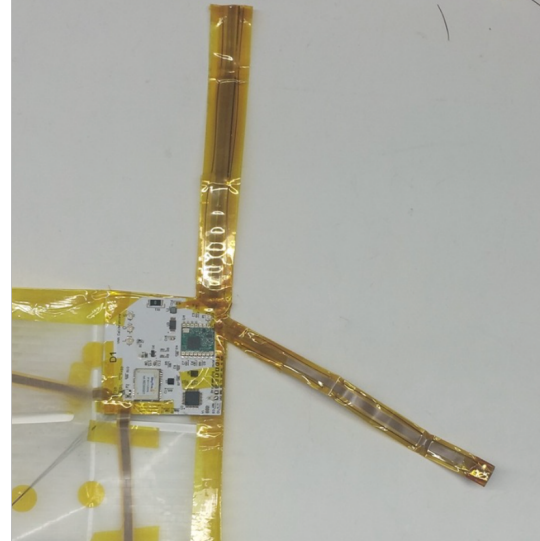


Figure 13: Hinged antenna design on the sail in the flight configuration.

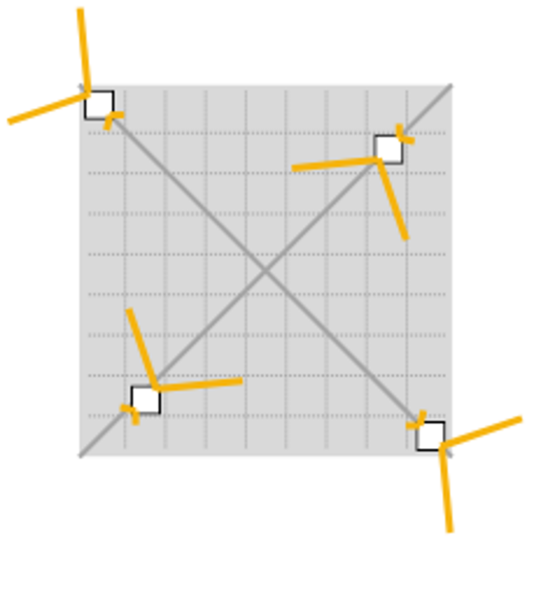


Figure 14: Configuration of the four ChipSats on the sail.

Although electrically, four-hinged antennas work, we were unable to use four of the hinged antennas because the sail stack was too thick to fit in the CubeSat compartment. A combination of the two designs, hinged and flexible, provided sufficient room in the sail stack, minimized interference, and kept deployment as passive and straightforward as possible. It also mitigated the risk of a failure from a singular type of design and introduced redundancy. Ideally, only two ChipSats are needed with solar panels on opposing faces of the sail because at least one ChipSat solar panel must be facing the Sun at any given position.

4.1. Long-Range High Altitude Balloon Test

With the final antenna configuration selected, we needed a test environment that would validate the antennas' ability to transmit data over long distances. A high-altitude balloon test served as a near-space testbed for these conditions. Through the University of Maryland's high-altitude balloon program, we launched our light sail system in a flight-like configuration (Figure 15).

The sail was flat-packed, with ChipSats and their antennas mounted exactly as they would be in the final deployment. Prior to this, the sail was stowed in the CubeSat for several days to more closely mimic the conditions of the real mission. This test allowed us to assess communication range and signal strength without requiring access to a full spaceflight mission.

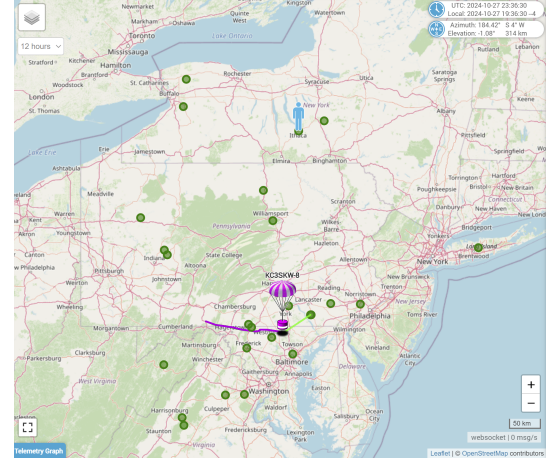


Figure 15: Trajectory of the high altitude balloon shown in purple/green with the blue figure indicating our location over 300km north.

```
[SX1278] CRC error!
1363.79,1,-34.69,-77.16,27410.00,-5.00,-1.00,6.00,-0.10,-0.10,-0.10,69.00,-2.00,-38.00,2.00,-13
0.00,-1.00,6.00,-0.10,-0.10,-0.10,69.00,-2.00,-38.00,2.00,-13
1364.12,1,39.67,-77.16,27410.00,-5.00,-1.00,6.00,-0.10,-0.10,-0.10,69.00,-2.00,-38.00,2.00,-13
5.75 dBm,-15.75 dB
[SX1278] CRC error!
[SX1278] CRC error!
[SX1278] CRC error!
[SX1278] CRC error!
1958.18,1,39.66,-77.64,13610.00,245.00,18.00,-80.00,0.00,0.00,-0.10,75.00,10.00,-18.00,-20.00,
-127.75 dBm,-12.75 dB
[SX1278] CRC error!
1993.96,1,39.66,-77.83,13850.00,147.00,64.00,-57.00,0.00,0.00,-0.10,75.00,8.00,-1.00,-21.00,-1
32.25 dBm,-15.25 dB
2006.38,1,39.64,-77.82,12850.00,245.00,-9.00,-76.00,-0.10,0.10,-0.20,76.00,-15.00,-1.00,-22.00
-127.75 dBm,-12.75 dB
2028.24,1,39.66,-77.81,12520.00,122.00,-48.00,18.00,0.00,-0.10,-0.31,75.00,9.00,0.00,-23.00,-1
32.25 dBm,-15.25 dB
[SX1278] CRC error!
[SX1278] CRC error!
[SX1278] CRC error!
[SX1278] CRC error!
2333.88,1,39.65,-76.91,8470.00,89.00,8.00,4.00,-0.10,-0.10,0.00,73.00,11.00,-6.00,-25.00,-131.
75 dBm,-12.75 dB
2342.41,1,39.65,-76.88,7970.00,77.00,60.00,41.00,-0.10,-0.10,-0.10,73.00,14.00,-16.00,-25.00,-1
32.25 dBm,-15.25 dB
2370.36,1,39.65,-76.88,7970.00,118.00,58.00,-17.00,0.00,-0.10,-0.10,73.00,-10.00,-26.00,-24.00
,-135.00 dBm,-17.00 dB
```

Figure 16: Antenna log during descent, where CRC errors indicate expected data corruption due to decreasing signal quality induced by attenuators.

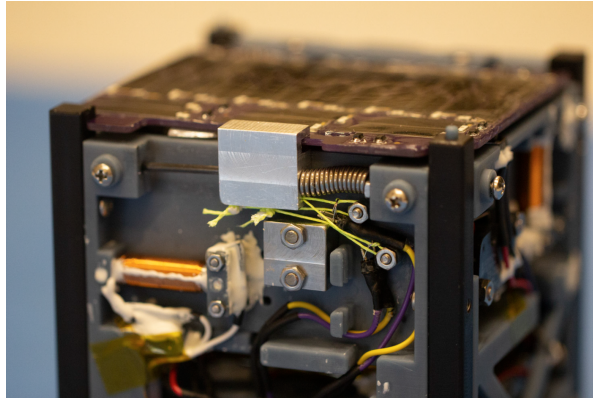


Figure 17: Latch held back by two fishing line wires (neon).

On the ground, we set up a receiving station with two Yagi antennas and two ground-plane antennas. We primarily intended to test the transmission capability of the LoRa antennas. This was successful, as we received packets from three of the four ChipSats. GPS data was also obtained from two ChipSats, confirming that the GPS antenna design is also functional. GPS data is not mission-critical and the antennas suffered RF interference from battery packs on the balloon payload, so receiving GPS from any of the ChipSats was promising news.

We assessed signal strength through an attenuation test simulating levels equivalent to the expected signal loss at orbital altitude and continued to receive packets from all ChipSats (Figure 16). While not a perfect mockup of spaceflight, the balloon test provided valuable pre-launch confidence that both GPS and LoRa antennas would operate effectively after deployment in the chosen configuration.

5. System-Level Integration

Now that both the light sail-ChipSat integration and CubeSat assembly were finalized, the last major task was final integration of the payload with the CubeSat bus. The light sail is deployed from a compartment inside the CubeSat, which is closed by a spring-loaded door.

Premature deployment had to be avoided at all costs, as ejecting the sail inside the deployer or near the ISS would pose a serious safety risk. To prevent this, we focused our integration efforts on the burn-wire latch mechanism that secures the door.

The latch is held in place by two Dyneema® fishing lines, each tensioned and wrapped around its own

nichrome burn wire (Figure 17). When the wires are activated, they heat up and sever the lines, releasing a spring-loaded latch and allowing the door to open and the light sail to deploy.

Tying the fishing lines proved deceptively difficult. The knots needed to be tight enough to withstand vibration and long-term storage, yet clean and compact to avoid tangling, loosening, or catching on nearby hardware. The available working space was extremely limited, just a few centimeters between CubeSat components, making the process physically awkward and difficult to repeat consistently.

Given the mechanism's mission-critical nature, we rehearsed the process repeatedly. Over several weeks, we practiced tying the same knot, refining both our tying technique and how we held and tensioned the line. Once we had a repeatable method, we tested the full deployment system with the sail stowed, checking for slippage under load. We also tied a reference knot in the EDU unit and left it in place to track any movement or degradation from the time of handover through shipping and storage. In the final week before vibration testing, two full deployment tests were conducted on the real Flight Unit prior to the final tying of the fishing lines. These rehearsals helped validate the entire release chain and ensured the sail would deploy only under the correct conditions.

6. System-Level Testing

6.1. Software

Testing of flight software, while critical for any spacecraft, represented a particular focus during the Alpha CubeSat development cycle due to the comparatively high number of software-based failure modes that a mechanically simple spacecraft can be exposed to, even without common failure points such as deployables. This can be attributed in part to the harsh and dynamic nature of spaceflight, as well as the inability to take corrective action should a software bug result in a loss of communication with the spacecraft. Additionally, student-led CubeSat teams like Alpha face challenges in reliably capturing all test cases and mission risks, with factors like turnover of graduating members with deep architecture knowledge.

To combat these risks, the software team implemented a milestone-gated, HITL-focused approach to software integration and testing, with mission-readiness increasing at critical intervals through handover of the spacecraft to Nanoracks in March 2025.

Following the development and testing described in the previous paper [3], and after approximately another



Figure 18: Alpha team celebrates completion of 18 hour flight software code review.

year of software development and feature additions, a line-by-line code review was conducted over an 18-hour period in January 2024, with the intention of addressing major areas that may have been overlooked during compartmentalized subsystem development.

This review led to critical fixes to the radio control logic, as well as improvements to the mission mode sequence and sensor reading logic, among other areas. It also put the team in a good place to conduct CBCS (Computer-Based Control System) testing over the Spring 2024 semester, which verified that the flight software met basic NASA and Nanoracks safety and functionality requirements. Significant testing was also performed on the CubeSat's attitude control software, documented in more detail in [4].

Following this testing, Alpha spent the last approximately eight months in a phase of rigorous day-in-the-life testing, which covered a variety of anticipated nominal, off-nominal, and emergency situations. A focus was placed on power budget testing, accomplished using a setup with dual benchtop flatsats, solar simulators, and satellite-connected RockBLOCK radios for maximum fidelity. An example data set from a power budget test is shown in Figure 19.

Utilizing this apparatus with remote access software, the software team was able to test multiple mission scenarios simultaneously, 24/7, for several months. During this time, remaining bugs and low-risk, high-benefit features were also added, such as the capability to selectively disable electrical components for power reasons or tune deployment conditions based on environmental data downlinked on-orbit.

Ultimately, testing concluded with successful end-to-end testing of the mission sequence and deployment

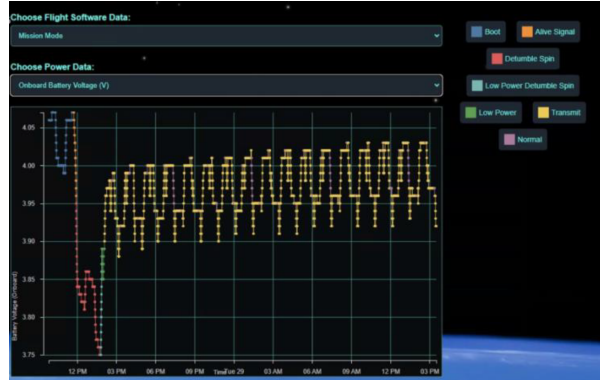


Figure 19: Increasing voltage during day-in-the-life HITL testing indicates positive power budget charging CubeSat battery.

process on both an EDU and the Flight hardware — testing opportunities not usually afforded to larger and more complex spacecraft — the completion of which places Alpha flight software in a state of flight readiness and concludes what was a five-year journey from pseudocode to flight software.

6.2. Vibration Test

Launch introduces significant vibrational loads across all axes of the spacecraft, so we conducted both informal and formal vibration tests to validate that the sail assembly and antennas could withstand the flight conditions. We began with informal tests designed to confirm that the hardware would not break, shift, or interfere with deployment, and to ensure the sail latch would not accidentally deploy due to launch vibrations. The formal vibration test within the Nanoracks deployer was also a requirement for launch approval.

Our initial tests utilized an informal paint shaker setup (Figure 20), with the CubeSat mounted in the location where the paint can would typically be positioned. We folded the sail with the antenna designs installed and secured the CubeSat inside the shaker. The goal was to identify and address obvious mechanical issues, such as loose screws, loose antenna connections, or the sail catching on the walls of the compartment during deployment. We also wanted to see if vibration would stress solder joints or shear antenna legs near the pad. Additionally, we checked the photovoltaic solar cells on the sail door to ensure they had not cracked and that the power generated remained consistent before and after the test.

Later in the semester, we completed a formal vibration test at Intertek in Cortland, NY as part of Voyager's

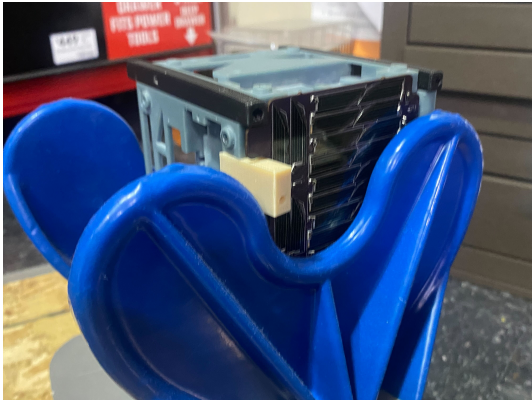


Figure 20: CubeSat prototype placed in the paint shaker setup with the light sail inside.

certification process. The CubeSat was tested on different faces using standard launch vibration profiles based on the GEVS standards used for CubeSats launched to the ISS (Figure 21). This test was crucial for verifying that the CubeSat could survive the flight environment without the sail compartment latch opening early, hardware shaking loose inside the deployer, or wire harnesses loosening. We paid close attention to small fasteners, conformal coating, and any loose debris.

After the vibration test, we verified that the CubeSat sensor data readouts were consistent, that magnetoquers were operational, and that the RockBLOCK radio continued to transmit successfully. These post-test checks confirmed that the critical subsystems had not been disrupted by launch-like vibrational loads. Although the CubeSat was already in a late stage of integration, which made it impractical to disassemble and visually inspect the internals, we relied on several layers of confidence. Earlier informal vibration tests had not revealed any major mechanical or electrical issues, and our final build followed a rigorously rehearsed and documented assembly procedure. This minimized the risk of loose fasteners, broken solder joints, or compromised wiring within the stack. Our structured approach to flight assembly gave us high confidence that the CubeSat was still fully functional.

6.3. Thermal Vacuum Test

The thermal vacuum chamber (TVC) test was one of the final steps in validating our assembled flight hardware. Although many individual components had already been tested in isolation, this was our chance to see how the full stack behaved in a space-like environment, both thermally and under vacuum. The Space Systems



Figure 21: Vibration test of Alpha CubeSat in NCRSD soft-stow configuration at the Intertek facility

Design Studio houses its own vacuum chamber. After significant efforts by the mechanical subteam to restore the chamber to full operation in early 2023, the completed CubeSat Flight Unit was thoroughly tested to high and low temperatures in vacuum prior to permanent assembly.

Following permanent assembly and vibration, the team conducted final thermal-vacuum testing. The main goals were to confirm that nothing degraded under thermal stress, that the sail compartment latch didn't slip from its compressed state under the tension of the fishing line (Figure 17), and that the sail door remained securely closed. We also watched for any peeling from conformal coating or adhesives, which could reduce solar power generation or interfere with deployment. As a rideshare on the CubeSat, holographic artwork is mounted over the solar panels. A thick layer of conformal coating is used to encapsulate these holograms and adhere them to PV panel, posing additional risk for power generation should any peeling occur.

The TVC has two parts that we control: the temperature of the heat exchanger plate, which is cooled by liquid nitrogen, and halogen lamps to simulate the heat from the sun (Figure 23). The CubeSat is secured in the chamber with thermocouples attached to key components, including the sail compartment latch, solar panels, CubeSat rails, and the Accura® Bluestone™ chassis. We monitored temperature responses across these locations throughout the test duration. Pictures of the CubeSat before and after were taken to ensure that all changes to the CubeSat were noticed and analyzed. It was observed that a small amount of conformal coating had lifted off the corner of one of the solar panel PCBs and was safely shaved off to mitigate additional peeling.

In the final tests prior to CubeSat delivery, we tested the sail compartment spring-latch mechanism. We were



Figure 22: Thermal vacuum chamber setup in SSDS.

concerned whether the fishing line holding back the latch would creep significantly after prolonged exposure to thermal stress and vacuum. The CubeSat was cooled to -10C before heating to +40C internally and +80C externally. Sub-millimeter creep was observed in the fishing line and deemed acceptable for flight. During the long-term storage between this test and the team's final view of the CubeSat three months later, negligible creep occurred and provided a strong indication of the integrity of the latch mechanism for launch.

The other significant issue was the expansion of gas bubbles underneath the holograms on the solar panels, which blurred the surface and could have rendered them unusable for generating power. Using a small syringe, small relief holes were added in the holographic film to mitigate future issues.

TVC testing served as a real-world check on both the mechanical tolerancing and integration of the system. Even small effects like latch creep over time or unexpected peeling had to be caught and addressed before flight. These were not issues we could solve at the component level; they only showed up once everything was assembled and placed in a realistic environment. Running a full cycle in the chamber gave us the confidence that the flight unit would be able to survive.

7. Final Integration

Following the vibration test and final software tests, the CubeSat was carefully packaged and driven to Houston for integration. Final checkouts included a physical inspection of the satellite for any damage to the solar panels, a top-up of the batteries, and a brief check of



Figure 23: Alpha CubeSat inside thermal vacuum chamber with thermocouples mounted for testing.



Figure 24: Joshua Umansky-Castro sliding Alpha CubeSat into the NRCSD in the Voyager Space cleanroom in Houston, Texas.

the flight computer's serial logs to confirm all sensors were functioning. A compass helped identify a stable magnetic field in the cleanroom where the magnetometer readings could be verified. Following a final set of deployment switch toggles and deployer fit checks, the CubeSat was slotted into the NRCSD with three other 1Us flying onboard the NG-22 launch (Figure 24). After final goodbyes from the CubeSat developers, Voyager Space engineers removed all RBF tags and sealed up the deployer for handover to NASA.

8. Future Work

Alpha CubeSat is slated for a Fall 2025 launch and a late 2025 deployment from the ISS. Until then, several activities are planned for alternative sail deploy demos. These tests include a demonstration within the microgravity environment of the space station as well as a high altitude balloon sail deployment. Ground station preparation and continued mission operation rehearsals are also scheduled in anticipation of the mission start date.

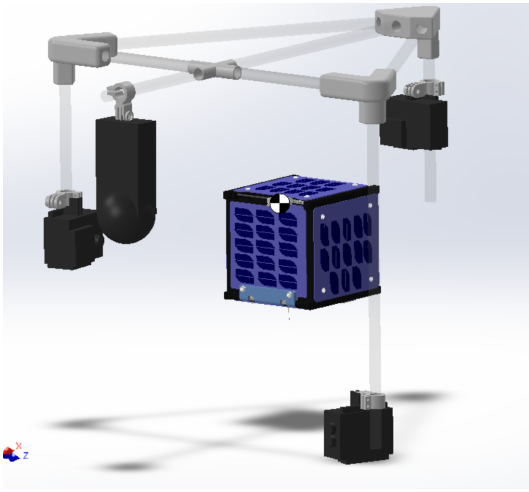


Figure 25: CubeSat High Altitude Balloon experiment with camera mounting rig.

8.1. High Altitude Balloon Sail Deployment

The CubeSat has communication capabilities but can only downlink low-resolution optical data on a periodic basis. There is no way to capture video of the deployment in orbit. To get footage of the CubeSat ejecting the sail in a space-like environment, the Alpha Team started work on the high-altitude balloon (HAB) project, as well as an ISS sail deploy demo that is further detailed in [5]. The Balloon CubeSat will have all the sensory and power capabilities of the orbital CubeSat, but it will not have an attitude control system due to the high-spin nature of the HAB platform. The Balloon CubeSat will be launched in a launch rig equipped with cameras, as shown in Figure 25. The backend development of all flight software systems has been completed.

The avionics board hosts a variety of sensory and communication systems that were tested and programmed for the flight mission. The approach taken was to verify the electrical design functionality of the new board, as well as the code used to execute the mission. Integration between the electrical and software systems, with the mechanical assembly of the balloon rig has been started. The sensory systems have all been validated. The development of a ground station specifically for the balloon mission facilitates user interaction with the flight software. It would be a user interface that allows for the transmission of commands, the display of normal report packages, and the compilation and display the fragmented images.

The balloon mission serves as both a technical testbed and a hands-on training platform. It enables us to val-

idate our electrical and software systems in a flight-like environment where communications are real, power budgets are critical, and telemetry must function under actual atmospheric conditions. At the same time, it provides newer team members with a lower-risk opportunity to walk through integration, testing, and mission operations without the pressure of spaceflight. Though the balloon unit will not have full attitude control hardware, it's built to match the orbital CubeSat's radio and sensory systems as closely as possible, and the payload is designed to capture the sail deployment on camera. The result is a realistic dry run of flight operations that feeds directly into confidence for future missions.

The Alpha Team is targeting a Fall 2025 balloon launch that would occur prior to our actual CubeSat mission start.

9. Lessons Learned

Across every subsystem, one of the most consistent takeaways was how often small issues, initially assumed to be minor, became critical when the system was fully integrated. Antenna designs that worked well in isolation introduced unexpected problems, such as frequency shifts, mechanical shearing, and mutual interference, once they were placed in close proximity and subjected to folding. These failures were only exposed when we tested the complete system, with all antennas mounted, the sail folded, and the CubeSat stowed as it would be in orbit.

Mechanical systems required the same level of scrutiny. Parts that seemed mechanically solid under casual testing encountered issues once tolerances were stacked or thermal stresses were introduced. Those kinds of problems required physical iteration and attention to small details, such as sanding down fit surfaces or inspecting edges.

Vibration testing also reinforced how easily critical failures can be introduced by minor oversights. Items such as loose screws, flakes of conformal coating, or cable slack can compromise performance or even prevent deployment. In a system as compact and interdependent as a 1U CubeSat, careful procedure is just as important as design quality.

The most reliable results came not from component-level tests, but from validating the final flight configuration under realistic conditions. Successful integration required not just functioning parts, but confidence in how they would behave together through every stage of the mission.

10. Conclusion

Bringing Alpha to a flight-ready state required a shift from isolated testing to fully integrated systems engineering. Throughout the process, we encountered issues that only emerged when subsystems were combined: interference between antennas, mechanical failures during deployment, and tolerance stackups across structural components. Solving these required detailed design revisions, extensive hardware testing, and thorough assembly procedures. On the software side, integration efforts focused on validating flight-critical tasks, such as command handling and power management. Vibration and thermal vacuum tests confirmed that the CubeSat can survive the launch and space environment, while the balloon tests provide a realistic check on deployment and communication performance. With these results, we have high confidence that the current configuration meets the necessary requirements for launch and operation on orbit.

Acknowledgements

The authors would like to thank our advisor and mission PI, Prof. Mason Peck, for creating the opportunity and supporting our continued work on this project. The launch opportunity is made possible through the NASA CubeSat Launch Initiative, and the dedicated efforts of Voyager Space (formerly Nanoracks) and Sterk Solutions. We are forever grateful for the many crowdfunding donors and generations of SSDS students that have helped bring this project to the launchpad. On the I&T team, special thanks to Marcus Esposito '24 for his dedication to resolving the final issues with the deployment switch plungers and Deemo Chen '24 for his frequent resin prints of the plunger iterations. We are especially indebted to I&T lead Millie Schwartz '23, for her dedication over numerous weekends to diagnose and remove leaks from our thermal vacuum chamber, enabling the critical testing needed for flight readiness. Thank you to Nikhil Agashe at Avery Dennison, Reflective Solutions, for the light sail material. Time on this project is additionally provided by generous funding from the Sloan, Cornell Colman, and GEM fellowships.

References

- [1] Joshua Umansky-Castro et al. Design of the alpha cubesat: Technology demonstration of a chipsat-equipped retroreflective light sail. In *AIAA SciTech 2021 Forum*, 01 2021. doi: 10.2514/6.2021-1254.
- [2] Joshua Umansky-Castro et al. Gram-scale chipsat spacecraft for light sailing in leo. *Annual AIAA/USU Conference on Small Satellites, Salt Lake City, UT; United States*, August 2025.
- [3] Joshua Umansky-Castro et al. The maker's cubesat: Increasing student-lab capabilities in the design, integration test of the alpha cubesat. *Annual AIAA/USU Conference on Small Satellites, Logan, UT; United States*, August 2022.
- [4] Joshua Umansky-Castro et al. Cots implementation of magnetorquer-only cubesat spin stabilization. *Annual AIAA/USU Conference on Small Satellites, Salt Lake City, UT; United States*, August 2025.
- [5] Verena Padres et al. Sailing to the stars: Free-flying light sails in microgravity. *Annual AIAA/USU Conference on Small Satellites, Salt Lake City, UT; United States*, August 2025.